NASA/CR-1999-209553
ICASE Report No. 99-37

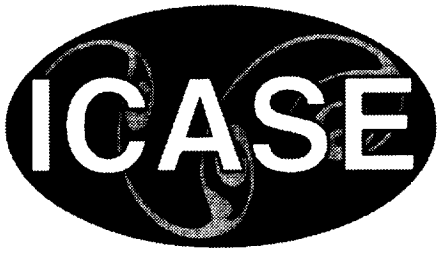


# Towards Understanding the Mechanism of Receptivity and Bypass Dynamics in Laminar Boundary Layers

*D.G. Lasseigne*
*Old Dominion University, Norfolk, Virginia*

*W.O. Criminale*
*University of Washington, Seattle, Washington*

*R.D. Joslin*
*NASA Langley Research Center, Hampton, Virginia*

*T.L. Jackson*
*University of Illinois, Urbana, Illinois*


September 1999

## *The NASA STI Program Office . . . in Profile*

Since its founding, NASA has been dedicated to the advancement of aeronautics and space science. The NASA Scientific and Technical Information (STI) Program Office plays a key part in helping NASA maintain this important role.

The NASA STI Program Office is operated by Langley Research Center, the lead center for NASA's scientific and technical information. The NASA STI Program Office provides access to the NASA STI Database, the largest collection of aeronautical and space science STI in the world. The Program Office is also NASA's institutional mechanism for disseminating the results of its research and development activities. These results are published by NASA in the NASA STI Report Series, which includes the following report types:

- TECHNICAL PUBLICATION. Reports of completed research or a major significant phase of research that present the results of NASA programs and include extensive data or theoretical analysis. Includes compilations of significant scientific and technical data and information deemed to be of continuing reference value. NASA counter-part or peer-reviewed formal professional papers, but having less stringent limitations on manuscript length and extent of graphic presentations.

- TECHNICAL MEMORANDUM. Scientific and technical findings that are preliminary or of specialized interest, e.g., quick release reports, working papers, and bibliographies that contain minimal annotation. Does not contain extensive analysis.

- CONTRACTOR REPORT. Scientific and technical findings by NASA-sponsored contractors and grantees.

- CONFERENCE PUBLICATIONS. Collected papers from scientific and technical conferences, symposia, seminars, or other meetings sponsored or co-sponsored by NASA.

- SPECIAL PUBLICATION. Scientific, technical, or historical information from NASA programs, projects, and missions, often concerned with subjects having substantial public interest.

- TECHNICAL TRANSLATION. English-language translations of foreign scientific and technical material pertinent to NASA's mission.

Specialized services that help round out the STI Program Office's diverse offerings include creating custom thesauri, building customized databases, organizing and publishing research results . . . even providing videos.

For more information about the NASA STI Program Office, you can:

- Access the NASA STI Program Home Page at http://www.sti.nasa.gov/STI-homepage.html

- Email your question via the Internet to help@sti.nasa.gov

- Fax your question to the NASA Access Help Desk at (301) 621-0134

- Phone the NASA Access Help Desk at (301) 621-0390

- Write to:
  NASA Access Help Desk
  NASA Center for AeroSpace Information
  7121 Standard Drive
  Hanover, MD 21076-1320

NASA/CR-1999-209553
ICASE Report No. 99-37

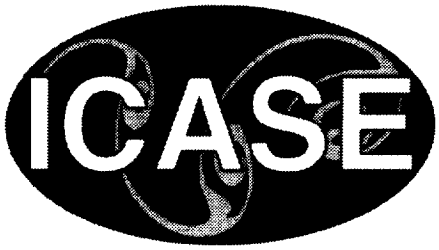


# Towards Understanding the Mechanism of Receptivity and Bypass Dynamics in Laminar Boundary Layers

*D.G. Lasseigne*
*Old Dominion University, Norfolk, Virginia*

*W.O. Criminale*
*University of Washington, Seattle, Washington*

*R.D. Joslin*
*NASA Langley Research Center, Hampton, Virginia*

*T.L. Jackson*
*University of Illinois, Urbana, Illinois*

*Institute for Computer Applications in Science and Engineering*
*NASA Langley Research Center, Hampton, VA*
*Operated by Universities Space Research Association*


National Aeronautics and
Space Administration

Langley Research Center
Hampton, Virginia 23681-2199

Prepared for Langley Research Center
under Contract NAS1-97046

September 1999

Available from the following:

NASA Center for AeroSpace Information (CASI)
7121 Standard Drive
Hanover, MD 21076-1320
(301) 621-0390

National Technical Information Service (NTIS)
5285 Port Royal Road
Springfield, VA 22161-2171
(703) 487-4650

# TOWARDS UNDERSTANDING THE MECHANISM OF RECEPTIVITY AND BYPASS DYNAMICS IN LAMINAR BOUNDARY LAYERS*

D.G. LASSEIGNE†, W.O. CRIMINALE‡, R.D. JOSLIN§, AND T.L. JACKSON¶

**Abstract.** Three problems concerning laminar-turbulent transition are addressed by solving a series of initial value problems. The first problem is the calculation of resonance within the continuous spectrum of the Blasius boundary layer. The second is calculation of the growth of Tollmien-Schlichting waves that are a direct result of disturbances that only lie outside of the boundary layer. And, the third problem is the calculation of non-parallel effects. Together, these problems represent a unified approach to the study of freestream disturbance effects that could lead to transition. Solutions to the temporal, initial-value problem with an inhomogeneous forcing term imposed upon the flow is sought. By solving a series of problems, it is shown that:

- A transient disturbance lying completely outside of the boundary layer can lead to the growth of an unstable Tollmien-Schlichting wave.
- A resonance with the continuous spectrum leads to strong amplification that may provide a mechanism for bypass transition once nonlinear effects are considered.
- A disturbance with a very weak unstable Tollmien-Schlichting wave can lead to a much stronger Tollmien-Schlichting wave downstream, if the original disturbance has a significant portion of its energy in the continuum modes.

**Key words.** boundary layer, receptivity

**Subject classification.** Fluid Dynamics

**1. Introduction.** In previous work [3],[8], the authors have shown a strong correlation to the solution of a temporal, three-dimensional, initial-value problem and the direct numerical simulation of the spatial problem. The methodology consisted of solving the linear disturbance equations subject to a series of initial values. These solutions are relatively easy, fast, and inexpensive to calculate. The corresponding spatially evolving flow was then determined by direct numerical simulation using the full Navier-Stokes equations and the two solutions were compared. During the period of transient growth for both channel flow and the laminar boundary layer, the two approaches agree quite well. Thus, it is reasonable to use the inexpensive and fast solutions of the temporal, initial-value problem as a means to conduct numerical experiments that can lead to greater understanding of receptivity and bypass mechanisms. Of course, the suitability of this approach must be continually confirmed by selectively using the more expensive direct numerical simulation to compare with the major results. For channel flow [3], the dynamics of specific initial conditions were determined, and the growth of disturbance energy compared to initial conditions which produce optimal growth of disturbance energy. The optimal initial conditions were determined by appropriately expanding the initial condition, finding the solution to a relatively few number of initial value problems, and determining

*This research was supported by the National Aeronautics and Space Administration under NASA Contract No. NAS1-97046 while the first, second, and fourth authors were in residence at the Institute for Computer Applications in Science and Engineering (ICASE), NASA Langley Research Center, Hampton, VA 23681-2199.

†Department of Mathematics and Statistics, Old Dominion University, Norfolk, VA 23529

‡Department of Applied Mathematics, University of Washington, Seattle, WA 98195

§Fluid Mechanics and Acoustics Division, NASA Langley Research Center, Hampton, VA 23681-2199

¶Center for Simulation of Advanced Rockets, University of Illinois, Urbana, IL 61801

the coefficients which maximized the disturbance energy. The transient period of the laminar boundary layer [8] was investigated in a similar manner. By using this approach, the contributions of the continuum modes are properly assessed, and it is determined that they must play a crucial role in the analysis of bypass mechanisms. It is only natural that we extend our studies to investigate the effects that freestream disturbances have on the laminar boundary layer.

Receptivity has traditionally been divided into two broad categories, forced receptivity or natural receptivity, based on the physical and mathematical descriptions. Forced receptivity is characterized by the experiments of Nishioka and Morkovin [9] where disturbances of limited spatial extent are introduced in the freestream *downstream* of the leading edge. The case of natural receptivity is characterized by the experiments of Boiko, *i.e.*,[1] where a disturbance field *upstream* of the leading edge of a smooth plate is generated. Great care is used to establish a zero pressure gradient at the plate, so that the mean flow (in the absence of the grid) has a Blasius profile. By assuming that disturbances are kept at a level in which linear theory applies, the differences between the two types of receptivity are seen mathematically in that the forced receptivity problem is governed by a set of inhomogeneous linear partial differential equations in time and space and natural receptivity by the homogeneous problem. Downstream of the imposed disturbance, the forced receptivity problem is the same mathematically as the natural receptivity problem. In addition to the two traditional categories of receptivity, there is a third case of receptivity that results in either an inhomogeneous problem or a homogeneous problem depending on the modeling approach taken. This case concerns the scattering of freestream disturbances by localized surface irregularities (*e.g.* acoustic disturbance or free stream turbulence with surface roughness or surface blowing and suction). Viewed as a perturbational problem, an inhomogeneous problem results; however, viewed as a problem of changing mean flow, a homogeneous problem results. Here, it is referred to as the naturally-forced receptivity problem since it has characteristics of both of the traditional categories.

The procedure used here, integrating the linear disturbance equations of temporal stability theory as an initial value problem, is straightforward and simple. It has already been demonstrated to be able to agree well with the direct numerical simulation of the spatial problem since in every numerical calculation, the complete solution – including the continuum eigenfunctions of the Orr-Sommerfeld problem and all discrete modes – is determined. Only afterwards is this solution interpreted in terms of the individual modes of the Orr-Sommerfeld equations. The theory of expanding the solution in terms of Orr-Sommerfeld eigenfunctions is presented in the classic work of Salwen and Grosch [10] while the description of the important continuum modes is found in Grosch and Salwen [6].

The rest of the paper is organized in the following manner. In Section 2, the equations governing the evolution of a disturbance under the assumptions of parallel linear theory and subjected to forcing terms are presented. The forcing terms can be interpreted as resulting from the forced receptivity problem or the nonlinear interaction of two linearly independent disturbances in the naturally forced receptivity problem. Fourier transforms in the streamwise and spanwise direction reduce the equations to partial differential equations in time and the vertical variable $y$. In the case of naturally forced receptivity, it is determined that the only part of the force that can affect the normal velocity component, and therefore the generation of Tollmien-Schlichting waves, is the divergence free component of the force. In Section 3, two major issues are explored by constructing the complete solutions of the temporal inhomogeneous problem using a model mean flow. The first issue deals with the difference between specifying the forcing by prescribing the individual forcing components in the momentum equations (naturally forced receptivity) or by specifying a vorticity source (forced receptivity). It is shown that by specifying the vorticity source, there is an immediate response

throughout the boundary layer which leads to a much higher degree of receptivity than the specification of forcing in the momentum equations. The second issue deals with the possibility of resonant forcing. Both these important issues are later addressed by numerical calculations using the continuous mean value profile, and the analytical results of this section are verified. In Section 4, the construction of the solution to the inhomogeneous problem in terms of all of the eigenfunctions of the Orr-Sommerfeld problem is presented. The gain in the coefficients of an eigenfunction expansion of the solution from before the imposition of forcing to after the imposition of the forcing is used to characterize the receptivity due to the forcing. Most importantly though, it is noted that the results after the imposition of the disturbance should be considered as initial values at a higher Reynolds number. Thus the transfer of the solution in terms of an Orr-Sommerfeld eigenfunction from one Reynolds number to another is presented. It is also shown in this section, that if the forcing is specified as forcing components in the momentum equations, that the eigenfunction expansion of the solution to the inhomogeneous problem has a simple form. From this solution, it is seen that the resonance found in Section 3 is indeed a resonance of the forcing with the continuum modes. All results presented in Section 4 are verified by numerical calculations.

**2. Basic Governing Equations.** For the flat-plate boundary layer, the fluid is taken as one of constant density with the basic flow approximated as parallel with $U = U(y), V = W = 0$. The instantaneous flow is decomposed into a basic state, $(U, V, W, P)$, plus a time-dependent disturbance to this basic state, (u,v,w,p). Then, the nondimensional linearized equations of motion are written as

$$\frac{\partial u}{\partial x} + \frac{\partial v}{\partial y} + \frac{\partial w}{\partial z} = 0, \tag{2.1}$$

$$\frac{\partial u}{\partial t} + U\frac{\partial u}{\partial x} + \frac{dU}{dy}v + \frac{\partial p}{\partial x} = R^{-1}\left[\frac{\partial^2 u}{\partial x^2} + \frac{\partial^2 u}{\partial y^2} + \frac{\partial^2 u}{\partial z^2}\right] + A, \tag{2.2}$$

$$\frac{\partial v}{\partial t} + U\frac{\partial v}{\partial x} + \frac{\partial p}{\partial y} = R^{-1}\left[\frac{\partial^2 v}{\partial x^2} + \frac{\partial^2 v}{\partial y^2} + \frac{\partial^2 v}{\partial z^2}\right] + B, \tag{2.3}$$

and

$$\frac{\partial w}{\partial t} + U\frac{\partial w}{\partial x} + \frac{\partial p}{\partial z} = R^{-1}\left[\frac{\partial^2 w}{\partial x^2} + \frac{\partial^2 w}{\partial y^2} + \frac{\partial^2 w}{\partial z^2}\right] + C. \tag{2.4}$$

The length scale chosen for non-dimensionalization is the displacement thickness, and thus the non-dimensional mean velocity is related to the Blasius boundary layer solution by $U(y) = f'(\delta_0^* y)$ with $f(\eta)$ being the solution to

$$f''' + \frac{1}{2}ff'' = 0 \qquad \text{subject to} \qquad f(0) = f'(0) = 0, \qquad f'(\infty) = 1. \tag{2.5}$$

where $\delta_0^* = \int_0^\infty (1 - f'(\eta))\, d\eta \approx 1.7208$. The nondimensional mean profile satisfies $\int_0^\infty (1 - U(y))\, dy = 1$ and $U(2.856) = .99$ gives the outer edge of the boundary layer. Here, $R$ is the conventional Reynolds number based on the displacement thickness, and time is nondimensionalized by the advective time scale. In addition, $A$, $B$ and $C$ are the nondimensional components of a prescribed force, $\vec{F}(x, y, z, t)$.

Then, by using the Fourier transformations defined with respect to $x$ and $z$ as

$$\breve{v}(\alpha, y, \beta, t) = \int_{-\infty}^{\infty}\int_{-\infty}^{\infty} v(x, y, z, t)e^{i(\alpha x + \beta z)}dxdz \tag{2.6}$$

(etc. for $u$,$w$, $p$, $A$, $B$ and $C$), equations (1) to (4) become

$$-i(\alpha\breve{u} + \beta\breve{w}) + \frac{\partial\breve{v}}{\partial y} = 0, \tag{2.7}$$

$$\frac{\partial\breve{u}}{\partial t} - i\alpha U\breve{u} + U'\breve{v} - i\alpha\breve{p} = R^{-1}\left[\frac{\partial^2\breve{u}}{\partial y^2} - \tilde{\gamma}^2\breve{u}\right] + \breve{A}, \tag{2.8}$$

$$\frac{\partial\breve{v}}{\partial t} - i\alpha U\breve{v} + \frac{\partial\breve{p}}{\partial y} = R^{-1}\left[\frac{\partial^2\breve{v}}{\partial y^2} - \tilde{\gamma}^2\breve{v}\right] + \breve{B}, \tag{2.9}$$

and

$$\frac{\partial\breve{w}}{\partial t} - i\alpha U\breve{w} - i\beta\breve{p} = R^{-1}\left[\frac{\partial^2\breve{w}}{\partial y^2} - \tilde{\gamma}^2\breve{w}\right] + \breve{C}, \tag{2.10}$$

respectively, where $U' = dU/dy$ and $\tilde{\gamma}^2 = \alpha^2 + \beta^2$. The Squire transformation, written as

$$\alpha\breve{u} + \beta\breve{w} = \tilde{\gamma}\tilde{u}, \tag{2.11}$$

$$-\beta\breve{u} + \alpha\breve{w} = \tilde{\gamma}\tilde{w}, \tag{2.12}$$

and combined with operations on (2.7) to (2.10) enables the elimination of the pressure to obtain the pair of equations

$$\left[\frac{\partial}{\partial t} - i\alpha U\right]\Delta\breve{v} + i\alpha U''\breve{v} = R^{-1}\Delta\Delta\breve{v} + i\left(\alpha\frac{\partial\breve{A}}{\partial y} + \beta\frac{\partial\breve{C}}{\partial y}\right) - \tilde{\gamma}^2\breve{B} \tag{2.13}$$

and

$$\left[\frac{\partial}{\partial t} - i\alpha U\right]\tilde{w} = \sin\phi U'\breve{v} + R^{-1}\Delta\tilde{w} - \sin\phi\breve{A} + \cos\phi\breve{C}, \tag{2.14}$$

where $\Delta$ is the linear operator

$$\Delta = \frac{\partial^2}{\partial y^2} - \tilde{\gamma}^2. \tag{2.15}$$

Here, $\sin\phi = \beta/\tilde{\gamma}$, $\Delta\breve{v}$ is proportional to the difference of the vorticity components in the $x - z$ plane ( $\Delta\breve{v} = i\beta\breve{\omega}_y - i\alpha\breve{\omega}_z$) and $\tilde{w}$ is proportional to the normal vorticity component ($\breve{\omega}_y = i\tilde{\gamma}\tilde{w}$). The first inhomogeneous term on the right hand side of (2.14) has been denoted as vortex tilting and acts as forcing for the normal vorticity. Such tilting is a product of the mean vorticity in the spanwise direction ($\Omega_z = -U'$) and the perturbation strain rate ($\partial v/\partial z$). For a three dimensional disturbance, the vortex tilting gives rise to the increase of the normal vorticity. It is clear that the solutions of (2.13) and (2.14), combined with continuity and the Squire transformation, are equivalent to solving (2.7) to (2.10). Lastly, $\breve{p}$ can be determined once the $\breve{v}$ component of velocity is known. In either case, solutions of the equations are subject to imposed initial conditions and the following boundary conditions at the the plate, namely

$$\breve{v}(0,t) = \frac{\partial\breve{v}}{\partial y}(0,t) = \tilde{w}(0,t) = 0, \tag{2.16}$$

as well as boundedness conditions in the freestream.

To evaluate the other velocity components, the quantities $\check{v}$ and $\check{w}$ are computed from (2.13) and (2.14), respectively. Then, the Squire transformation, (2.11) and (2.12), is inverted to give

$$\check{u} = -\frac{i\cos\phi}{\tilde{\gamma}}\frac{\partial\check{v}}{\partial y} - \sin\phi\ \check{w} \tag{2.17}$$

and

$$\check{w} = -\frac{i\sin\phi}{\tilde{\gamma}}\frac{\partial\check{v}}{\partial y} + \cos\phi\ \check{w}. \tag{2.18}$$

An energy density in the $(\tilde{\gamma},\phi)$ plane as a function of time is defined as

$$E^*(t) = \int_0^\infty \left[|\check{u}|^2 + |\check{v}|^2 + |\check{w}|^2\right] dy \tag{2.19}$$

or, in terms of the variables $\check{v}$ and $\check{w}$, this becomes

$$E^*(t) = \int_0^\infty \left[|\check{v}|^2 + |\check{w}|^2 + \tilde{\gamma}^{-2}\left|\frac{\partial\check{v}}{\partial y}\right|^2\right] dy. \tag{2.20}$$

In using these definitions, the class of disturbances is more restricted than those that are only bounded at infinity. However, in all calculations that follow, both the specified forcing and the initial conditions are chosen as decaying as $y \to \infty$ and therefore the energy integral defined as (2.20) converges for all time. The continuum is still represented in these calculations, as it is the *integral* over all the continuum modes, not an individual continuum mode that appears in the complete solution. The total energy of the perturbation can be found by integrating (2.20) over all $\tilde{\gamma}$ and $\phi$. A normalized energy density, namely

$$E(t) = \frac{E^*(t)}{E^*(0)}, \tag{2.21}$$

measures the growth in energy at time $t$ for a prescribed initial condition at $t = 0$ and subject to prescribed forcing.

**2.1. Interpretation of the Forcing: $\vec{F}$.** By knowing the perturbation velocity components, the perturbation vorticity is determined by appealing to their definitions, namely

$$\check{\omega}_x = \frac{\partial\check{w}}{\partial y} + i\beta\check{v}, \tag{2.22}$$

$$\check{\omega}_y = -i\beta\check{u} + i\alpha\check{w} \equiv i\tilde{\gamma}\check{w}, \tag{2.23}$$

and

$$\check{\omega}_z = -i\alpha\check{v} - \frac{\partial\check{u}}{\partial y}, \tag{2.24}$$

in wave space. The governing equations, (2.7) to (2.10), are recast into equations governing vorticity and pressure so that the effect the chosen forcing has on the flow can be interpreted. These equations are:

$$\left[\frac{\partial}{\partial t} - i\alpha U\right]\check{\omega}_x - i\alpha U'\check{w} = R^{-1}\Delta\check{\omega}_x + \frac{\partial\check{C}}{\partial y} + i\beta\check{B}, \tag{2.25}$$

$$\left[\frac{\partial}{\partial t} - i\alpha U\right] \check{\omega}_y - i\beta U' \check{v} = R^{-1}\Delta\check{\omega}_y - i\beta\check{A} + i\alpha\check{C}, \tag{2.26}$$

$$\left[\frac{\partial}{\partial t} - i\alpha U\right] \check{\omega}_z - i\beta U' \check{w} - U''\check{v} = R^{-1}\Delta\check{\omega}_z - \frac{\partial\check{A}}{\partial y} - i\alpha\check{B}, \tag{2.27}$$

and

$$\Delta\check{p} = 2i\alpha U'\check{v} - i(\alpha\check{A} + \beta\check{C}) + \frac{\partial\check{B}}{\partial y}. \tag{2.28}$$

The components of the force $\vec{F} = (A, B, C)$ are specified according to the particular problem at hand. Since any vector field can be decomposed into a field that is divergence free and a field that is curl free, and since the forcing terms in the vorticity and pressure equations are the curl and divergence of the force, respectively, this is a proper place to start. First, suppose that $\vec{F}$ represents the component of the force that is curl free, *i.e.*,

$$\nabla \times \vec{F} = 0. \tag{2.29}$$

In Fourier space this means

$$\frac{\partial\check{C}}{\partial y} + i\beta\check{B} = 0; \qquad \alpha\check{C} - \beta\check{A} = 0; \qquad i\alpha\check{B} + \frac{\partial\check{A}}{\partial y} = 0. \tag{2.30}$$

For this choice, the forcing terms appearing in the vorticity equations vanish, and only the pressure disturbance is directly affected. To specify this case, any one of the components of the force is considered as arbitrary while the other two components must satisfy (2.30).

Next, suppose that $\vec{F}$ represents the component of the force that is divergence free, *i.e.*,

$$\nabla \cdot \vec{F} = 0, \tag{2.31}$$

or, in Fourier space,

$$-i(\alpha\check{A} + \beta\check{C}) + \frac{\partial\check{B}}{\partial y} = 0. \tag{2.32}$$

Now, non-zero forcing terms appear only in the vorticity equations. To specify this case, two components of the force are considered as arbitrary while the last must satisfy (2.32). For convenience, the two independent modes of forcing in the normal velocity equation (2.13) without forcing in the normal vorticity equation (2.14) given by

$$\check{B} \neq 0, \qquad \text{and} \qquad -\beta\check{A} + \alpha\check{C} = 0 \tag{2.33}$$

and the opposite, forcing in the normal vorticity equation (2.14) without forcing in the normal velocity equation (2.13) given by

$$\check{B} = 0, \qquad \text{and} \qquad -\beta\check{A} + \alpha\check{C} = -\frac{\tilde{\gamma}}{\beta}\check{A}_0, \tag{2.34}$$

will be the only pair of divergence free forces considered. In the first instance, the forcing in (2.13) is the Laplacian of $B$.

**3. Complete Solution to an Inhomogeneous Model Problem.** It has been shown by Criminale and Drazin [2] that the viscous boundary layer problem can be solved analytically for large values of the Reynolds number by modeling the mean flow. This technique is particularly appropriate for studying boundary-layer free stream response to external forcing. In this limit, an outer layer, *i.e.*, the free stream, exists that approximates an irrotational flow of an inviscid fluid, an intermediate layer exists that approximates a rotational flow of an inviscid fluid, and a viscous sublayer exists at the plate. To leading order, the viscous terms are zero in the first two regions. The basic mean boundary layer flow is modeled as a uniform parallel stream above a uniform shear flow with a solid boundary below. Thus, for this entire section, the basic velocity is taken as

$$\vec{U}(y) = (U,0,0) = \begin{cases} (1,0,0) & y > 1 \\ \\ (y,0,0) & 0 < y \leq 1. \end{cases} \tag{3.1}$$

After substituting $\vec{U}$ from (3.1) and neglecting the viscous terms, the governing equations, (2.13) and (2.14), reduce to

$$\left[\frac{\partial}{\partial t} - i\alpha U\right] \Delta\breve{v} = i\left(\alpha\frac{\partial \breve{A}}{\partial y} + \beta\frac{\partial \breve{C}}{\partial y}\right) - \tilde{\gamma}^2\breve{B} \tag{3.2}$$

and

$$\left[\frac{\partial}{\partial t} - i\alpha U\right] \tilde{w} = \sin\phi\ U'\breve{v} - \sin\phi\ \breve{A} + \cos\phi\ \breve{C}, \tag{3.3}$$

which must be solved on either side of the interface located at $y = 1$ and coupled to the viscous sublayer below. Both the normal velocity $\breve{v}$ and the perturbation pressure

$$-\tilde{\gamma}^2\breve{p} = \left[\frac{\partial}{\partial t} - i\alpha U\right]\frac{\partial \breve{v}}{\partial y} + i\alpha U'\breve{v} - i(\alpha\breve{A} + \beta\breve{C}) \tag{3.4}$$

are required to be continuous at $y = 1$. The plate conditions where $\breve{v} = \breve{v}' = \tilde{w} = 0$ at $y = 0$ are secured by the solutions influenced by viscosity.

In what follows, a number of issues concerning the specification of the forcing in the vorticity equation will be resolved, and results of using models based on these concepts agree with the numerical results using the Blasius profile. These issues are directly related to whether the inhomogeneous terms represent the forced receptivity problems or the nonlinear interaction terms in the naturally forced receptivity problem. In the latter case, the inhomogeneous terms should be consistent with the velocity field since they have evolved along with the flow. In the former case, the externally applied forcing does not have to be consistent with a velocity field and this results in generation of vorticity at the plate. First, however, the issue of forcing in the pressure equation is examined.

**3.1. Forcing in the Pressure Equation.** In considering forcing due to pressure, the component of a force, $\vec{F}$, with curl equal to zero is all that is required. Therefore, for this analysis, it is assumed that $\nabla \times \vec{F} = 0$. The governing equations are

$$\left[\frac{\partial}{\partial t} - i\alpha U\right] \Delta\breve{v} = 0. \tag{3.5}$$

and

$$\left[\frac{\partial}{\partial t} - i\alpha U\right] \tilde{w} = \sin\phi\ U'\breve{v} \tag{3.6}$$

In like fashion, the equations for the vorticity ((2.25)-(2.27)) have no forcing terms. In short, unless vorticity is an input initially, it cannot be generated and solutions to (3.5) and (3.6) have only irrotational portions. The pressure equation does, on the other hand, have an extra term due to forcing and is

$$\Delta\check{p} = 2i\alpha U'\check{v} - i(\alpha\check{A} + \beta\check{C}) + \frac{\partial\check{B}}{\partial y}. \tag{3.7}$$

This relation can be cast in real space as well, namely

$$\nabla^2 p = -2U'\frac{\partial v}{\partial x} - \nabla\cdot\vec{F}. \tag{3.8}$$

Since $\nabla\times\nabla p = 0$ and defining

$$\nabla P = \nabla p + \vec{F}, \tag{3.9}$$

equation (3.8) becomes

$$\nabla^2 P = -2U'\frac{\partial v}{\partial x}. \tag{3.10}$$

Thus, $P$ plays the same role as $p$ when no external forcing in pressure is present. Seeing that this component of the forcing cannot generate vorticity, and therefore Tollmien-Schlicting waves, at this order of appoximation, attention is now focused on the divergence free component of the forcing terms.

**3.2. Naturally Forced Receptivity.** In this first subsection concerning the divergence free component of the forcing, the mathematically easier case of naturally forced receptivity is examined. The receptivity is not the result of a changing mean flow which will be studied numerically later as a homogeneous initial value problem, but rather the examination of a model of the forcing produced by the nonlinear interactions of two continuous disturbances (*e.g.*, acoustic disturbance or free stream turbulence with surface roughness or surface blowing and suction). As mentioned in the introduction, this problem has two different mathematical formulations depending on whether the problem is viewed as a perturbation series, or the disturbances caused by surface effects are included in the mean flow. The main feature of this type of forcing as opposed to forced receptivity, examined in the next subsection, is that the forcing terms are continuous and satisfy the same boundary conditions as the flow at the plate, *i.e.*, the forcing and its $y$ derivative are zero for $y = 0$. This means that the flow has evolved in such a way that there should not be any extra vorticity generated at the plate in order to compensate for the prescribed forcing. It is determined that in order to have this feature, the component $\check{B}$ of the force must be prescribed and not $\Delta\check{B}$. In the freestream and intermediate shear layer, the governing equations are

$$\left[\frac{\partial}{\partial t} - i\alpha U\right]\Delta\check{v} = \Delta\check{B}, \tag{3.11}$$

and

$$\left[\frac{\partial}{\partial t} - i\alpha U\right]\tilde{w} = \sin\phi U'\check{v} - \frac{\tilde{\gamma}}{\beta}\check{A}_0. \tag{3.12}$$

A Green's function for the solution for a single harmonic in time is developed by prescribing a delta function source. Since the solution differs depending on whether the force is in the freestream or the intermediate shear layer, both are developed at once by using

$$\check{B} = \Gamma_1(\alpha,\beta,\Omega_1,y_1)e^{i\Omega_1 t}\delta(y-y_1) + \Gamma_2(\alpha,\beta,\Omega_2,y_2)e^{i\Omega_2 t}\delta(y-y_2), \tag{3.13}$$

with $y_1 > 1$ so that a forcing in the freestream is represented, and $0 < y_2 < 1$ so that a forcing in the intermediate shear layer is represented. $\Omega_{1,2}$ are the nondimensional frequencies of the forcing and $\Gamma_{1,2}$ is a measure of the forcing amplitudes.

The solution is just simply

$$\breve{v} = \Gamma_1 \psi_1(t)\delta(y - y_1) + \Gamma_2 \psi_2(t)\delta(y - y_2), \tag{3.14}$$

where

$$\psi_1(t) = \begin{cases} \frac{e^{i\Omega_1 t} - e^{i\alpha t}}{i(\Omega_1 - \alpha)} & \text{if} \quad \Omega_1 \neq \alpha \\ \\ te^{i\alpha t} & \text{if} \quad \Omega_1 = \alpha, \end{cases} \tag{3.15}$$

and

$$\psi_2(t) = \begin{cases} \frac{e^{i\Omega_2 t} - e^{i\alpha y_2 t}}{i(\Omega_2 - \alpha y_2)} & \text{if} \quad \Omega_2 \neq \alpha y_2 \\ \\ te^{i\alpha y_2 t} & \text{if} \quad \Omega_2 = \alpha y_2. \end{cases} \tag{3.16}$$

Since the solution (3.14) automatically satisfies all boundary conditions, there is no need for an analysis of the viscous sublayer at this order.

Resonance is found to be possible when the nondimensional frequency $\Omega$ of the forcing is equal to the nondimensional wavenumber $\alpha$ times the value of the local nondimensional velocity. In dimensional terms, the resonance occurs whenever the forcing in the vorticity equations is advected with the flow.

After integrating Squire's equation (3.12) the general result becomes

$$\tilde{w} = \tilde{w}_0 e^{i\alpha U t} + \sin\phi \; U' \int_0^t \breve{v}(y, \bar{t}) e^{i\alpha U(t-\bar{t})} \, d\bar{t} - \int_0^t \frac{\tilde{\gamma}}{\beta} \breve{A}_0 e^{-i\alpha U(t-\bar{t})} d\bar{t} \tag{3.17}$$

valid both in the free stream and in the intermediate layer. In the freestream, where $U = 1$ and $U' = 0$, $\tilde{w}$ is independent of $\breve{v}$. The second integral of (3.17) shows resonance in the freestream occurs provided the forcing time dependence varies as

$$\breve{A}, \breve{C} \sim e^{i\alpha U t} = e^{i\alpha t}, \tag{3.18}$$

the same condition shown for resonance to occur for the $\breve{v}$ velocity component. Both the magnitudes of $\breve{v}$ and of $\tilde{w}$ increase linearly in time for this resonant mechanism. If forcing is in the intermediate layer and the nondimensional frequency of the streamwise and spanwise forcing is proportional to $\alpha U(y_2)$,

$$\breve{A}, \breve{C} \sim e^{i\alpha y_2 t}, \tag{3.19}$$

then the magnitudes again increase linearly in time. However, if the frequency of the spanwise vorticity forcing is $\Omega_2 = \alpha y_2$, the magnitude of $\breve{v}$ grows linearly in time, and the first integral of (3.17) shows the magnitude of $\tilde{w}$ increases quadratically in time at the location of the forcing, *i.e.*, at $y = y_2$. Thus, the energy will increase as rapidly as $t^4$ rather than $t^2$. Since any solution with fast growth might contribute to nonlinear interactions before the Tollmien-Schlichting waves become unstable, this resonance condition is important in the hunt for bypass mechanisms.

**3.3. Forced Receptivity.** Again, only the divergence free component of forcing is considered and the governing equation is (3.11). However, instead of specifying $\breve{B}$, one must specify $\Delta\breve{B}$. The consequences of this choice is that the analysis is much more involved since it must allow for generation of vorticity at the plate. Start by choosing

$$\Delta\breve{B} = \Gamma_1(\alpha,\beta,\Omega_1)e^{i\Omega_1 t}\delta(y-y_1) + \Gamma_2(\alpha,\beta,\Omega_2)e^{i\Omega_2 t}\delta(y-y_2), \tag{3.20}$$

with definitions of the constants the same as the previous subsection. The solution that meets the $y \to \infty$ boundary condition is

$$\breve{v} = \left(\breve{v}_1(y) - H(0)e^{-\tilde{\gamma}(y-1)}\right)e^{i\alpha t} + H(t)e^{-\tilde{\gamma}(y-1)} - \frac{\Gamma_1}{2\tilde{\gamma}}\psi_1(t)e^{-\tilde{\gamma}|y-y_1|}, \tag{3.21}$$

for $y > 1$ and

$$\breve{v} = \breve{v}_R(y,t) + D(t)e^{\tilde{\gamma}(y-1)} + E(t)e^{-\tilde{\gamma}(y-1)} + \frac{i\Gamma_2}{2\tilde{\gamma}}\psi_2(t)e^{-\tilde{\gamma}|y-y_2|}, \tag{3.22}$$

for $0 < y < 1$. The functions $\psi_{1,2}$ are the same as before. Here, $\breve{v}_R(y,t)$ satisfies the equation

$$\Delta\breve{v}_R = e^{i\alpha y t}\Delta\breve{v}_2, \qquad \breve{v}_R(y,0) = \breve{v}_2(y) - D(0)e^{\tilde{\gamma}(y-1)} - E(0)e^{-\tilde{\gamma}(y-1)}. \tag{3.23}$$

The quantities $\breve{v}_1$ and $\breve{v}_2$ are the initial conditions for $\breve{v}$ in the freestream and in the intermediate shear layer, respectively. The functions $H$, $D$ and $E$ are the coefficients of the homogeneous solution of $\Delta\breve{v} = 0$ (irrotational part of $\breve{v}$), and must be determined by matching with the solution of the intermediate main shear layer with the solution in the freestream at the interface $y = 1$ and with the viscous sublayer at $y = 0$. Since the time dependence is the same as before, the previous remarks about resonance and bypass also apply here.

The forcing has been set in the freestream or outer reaches of the boundary layer where viscosity is neglected. To complement this, a uniformly valid solution that does satisfy the boundary conditions where $\breve{v} = \breve{v}_y = \breve{w} = 0$ at $y = 0$ must be established and this requires viscosity near the plate. This was not necessary for the case of naturally forced receptivity where the solutions in the outer and inner layers automatically satisfied the boundary conditions. For the case of forced receptivity, solutions from a viscous sublayer must be found that satisfy the boundary conditions and then asymptotically matched to the solutions of the intermediate layer.

Near the plate, the governing equation for $\breve{v}$ is given by

$$\left(\frac{\partial}{\partial t} - i\alpha U\right)\Delta\breve{v} = \epsilon\Delta\Delta\breve{v}, \tag{3.24}$$

where $\epsilon = R^{-1}$.

The solution $\breve{v}$ is found by rescaling the vertical component $y$ in equations (3.24) as $Y = y/\sqrt{\epsilon}$ ($\tilde{\gamma} = O(1)$ at most). The leading order equation formed in the limit $\epsilon \to 0$ is

$$\frac{\partial}{\partial t}\left(\frac{\partial^2\breve{v}}{\partial Y^2}\right) = \frac{\partial^4\breve{v}}{\partial Y^4}. \tag{3.25}$$

A similarity solution of (3.25) for $\breve{v} = \sqrt{\epsilon}\breve{v}_Y$, where the amplitude factor is introduced in anticipation of matching, is sought which leads to the introduction of

$$\frac{\partial^2\breve{v}_Y}{\partial Y^2}(Y,t) = \Phi(\eta,\tau) \tag{3.26}$$

with $\eta = Y/2\sqrt{t}$ as the similarity variable and $\tau = t$. Then equation (3.25) becomes

$$4\tau\frac{\partial\Phi}{\partial t} - 2\eta\frac{\partial\Phi}{\partial\eta} - \frac{\partial^2\Phi}{\partial\eta^2} = 0. \tag{3.27}$$

Integrating (3.26) gives

$$\breve{v}_V = \int_0^Y \int_0^{Y'} \Phi(Y''/2\sqrt{t}, t)\, dY''\, dY' = \int_0^\eta \int_0^{\eta'} 4\tau\Phi(\eta'', \tau)\, d\eta''\, d\eta' \tag{3.28}$$

Upon using the Mellin transform of the function $\phi(\eta, \tau)$, defined as

$$\phi^M(\eta, s) = \int_0^\infty \tau^{s-1}\Phi(\eta, \tau)\, d\tau, \tag{3.29}$$

the Mellin transform of $\breve{v}_V$ and $\frac{\partial\breve{v}_V}{\partial Y}$ are determined to be

$$\breve{v}_V^M = \int_0^\eta \int_0^{\eta'} 4\Phi^M(\eta'', s+1)\, d\eta''\, d\eta', \tag{3.30}$$

and

$$\left(\frac{\partial\breve{v}_V}{\partial Y}\right)^M = \int_0^\eta 2\Phi^M(\eta'', s+\frac{1}{2})\, d\eta'. \tag{3.31}$$

At this stage, the function $\Phi$ (and therefore $\Phi^M$) is undetermined; however, the analysis can proceed by noting that the plate conditions have been met and $\Phi^M$ satisfies

$$\Phi^{M\prime\prime} + 2\eta\Phi^{M\prime} + 4s\phi^M = 0, \tag{3.32}$$

where primes denote derivatives with respect to $\eta$ holding $s$ constant. Since the solution must eventually match to the intermediate shear layer, the independent solution that behaves as $\phi^M \sim \eta^{2s}$ must be discarded and

$$\Phi^M(\eta, s) = C_1(s)\Phi_1(\eta, s), \tag{3.33}$$

with $\Phi_1$ being the independent solution of (3.32) with $\phi^M \sim e^{-\eta^2}$. With this solution, the quantity $(\frac{\partial\breve{v}_V}{\partial Y})^M$ is a function of $s$ as $\eta \to \infty$. Defining

$$V_1^M(s) = \int_0^\infty 2C_1(s+\frac{1}{2})\Phi_1(\eta'', s+\frac{1}{2})\, d\eta' \tag{3.34}$$

as the Mellin transform of the unknown function $V_1(t)$, the asymptotic form as $Y \to \infty$ of the viscous sublayer solution is

$$\breve{v}_V(Y, t) \sim V_1(t)Y + V_0(t). \tag{3.35}$$

The function $V_0$ is related to $V_1$ which is, in turn, determined by matching (3.30) with the intermediate layer solution (3.22). To achieve this matching requires

$$0 = \breve{v}_R(0, t) + D(t)e^{-\tilde{\gamma}} + E(t)e^{\tilde{\gamma}} - \frac{\Gamma_2}{2\tilde{\gamma}}\psi_2(t)e^{-\tilde{\gamma}y_2}, \tag{3.36}$$

and

$$V_1(t) = \breve{v}_{R_y}(0, t) + \tilde{\gamma}D(t)e^{-\tilde{\gamma}} - \tilde{\gamma}E(t)e^{\tilde{\gamma}} - \frac{\Gamma_2}{2}\psi_2(t)e^{-\tilde{\gamma}y_2}. \tag{3.37}$$

In like fashion the $\tilde{w}$ equation can be examined in the sublayer. The governing equation is

$$\left[\frac{\partial}{\partial t} - i\alpha U\right]\tilde{w} - \epsilon\Delta\tilde{w} = \sin\phi\, U'\check{v} \tag{3.38}$$

since there are no inhomogeneous terms due to forcing in this part of the boundary layer. By rescaling $Y = y/\sqrt{\epsilon}$ as before and letting $\tilde{w} = \sqrt{\epsilon}\,W$, the equation reduces in leading order to

$$\frac{\partial W}{\partial t} - \frac{\partial^2 W}{\partial Y^2} = \sin\phi\,\check{v}_V(Y,t) \tag{3.39}$$

which must be solved subject to $W(Y,0) = 0$ and $W(0,t) = 0$. Using the similarity variables and the Mellin transform $W^M(\eta,\tau)$, equation (3.39) becomes

$$W^{M\prime\prime} + 2\eta W^{M\prime} + 4sW^M = 4\sin\phi\,\check{v}_V^M(\eta, s+1). \tag{3.40}$$

The proper matching conditions are inferred from (3.40). Specifically, as $Y$ increases, the homogeneous solution that grows as $\eta^{2s}$ must be discarded and the homogeneous solution that decays as $e^{-\eta^2}$ is kept, but does not affect matching. The particular solution leads to linear growth in $Y$ dependent on the functions $V_1(t)$ and $V_0(t)$.

Assuming that the solution is started from zero initial conditions (*i.e.*, $\check{v}_1 = \check{v}_2 = 0$) leads to

$$\check{v}_R(y,t) = -D(0)e^{\tilde{\gamma}(y-1)} - E(0)e^{-\tilde{\gamma}(y-1)}. \tag{3.41}$$

Combining (3.36) and (3.37) leads to

$$E(t) - E(0) = -\frac{V_1(t)}{2\tilde{\gamma}}e^{-\tilde{\gamma}}, \tag{3.42}$$

and

$$D(t) - D(0) = \frac{V_1(t)}{2\tilde{\gamma}}e^{\tilde{\gamma}} - \frac{\Gamma_2}{2\tilde{\gamma}}e^{-\tilde{\gamma}(1-y_2)}\psi_2(t); \tag{3.43}$$

continuity of $\check{v}$ results in

$$H(t) = H(0)e^{i\alpha t} + \frac{\Gamma_1}{2\tilde{\gamma}}\psi_1(t)e^{\tilde{\gamma}(1-y_1)} + \frac{\Gamma_2}{2\tilde{\gamma}}e^{-\tilde{\gamma}(1-y_2)}\psi_2(t); \tag{3.44}$$

and continuity of $\check{p}$ at $y = 1$ results in

$$\begin{aligned}
&-\tilde{\gamma}\left(\dot{H}(t) - i\alpha H(t)\right) - \frac{\Gamma_1}{2}e^{\tilde{\gamma}(1-y_1)}\left(\dot{\psi}_1(t) - i\alpha\psi_1(t)\right) \\
&\qquad = \tilde{\gamma}\left(\dot{D}\ (t) - i\alpha(1 - \frac{1}{\tilde{\gamma}})(D(t) - D(0))\right) - \tilde{\gamma}\left(\dot{E}\ (t) - i\alpha(1 + \frac{1}{\tilde{\gamma}})(E(t) - E(0))\right) \\
&\qquad\qquad - \frac{\Gamma_2}{2}e^{-\tilde{\gamma}(1-y_2)}\left(\dot{\psi}_2\ (t) - i\alpha(1 + \frac{1}{\tilde{\gamma}})\psi_2(t)\right).
\end{aligned} \tag{3.45}$$

These last four equations constitute a system for the unknown functions $D(t)$, $E(t)$, $H(t)$ and $V_1(t)$. Thus, the unknown function from the wall layer, $V_1(t)$ is related to the forcing in the freestream and within the intermediate shear layer. At this point, a consistent solution for $\check{v}$ has been constructed. The solution for $\tilde{w}$ can also be constructed from (3.17) and automatically matches with the viscous sublayer solution. We note that the solutions exhibit resonance as in the case of the natural receptivity problem with the main difference between the two being that solutions for the forced receptivity problem immediately penetrate all the way to the plate even if the forcing is in the free stream. This highlights the elliptic components of the linear parallel disturbance equations. With this penetration into the boundary layer, it is expected that the forced problem leads to a much higher degree of receptivity than would the natural problem. This is confirmed by numerical calculations.

**4. Receptivity and Resonance.** From the previous section, we have seen that it is possible to excite the continuum by a resonance like behavior. Now the question to be asked is whether or not this can lead to receptivity? From the work of Salwen and Grosch [10], it is obvious that any arbitrary disturbance in the freestream has (mathematically) a small non-zero contribution from the discrete spectrum (*i.e.*, Tollmien-Schlichting waves). This was demonstrated numerically by Lasseigne *et al.*, [8] where the solution to the initial value problem with a disturbance localized about a point $y_0$ in the freestream produced an unstable Tollmien-Schlichting wave. An examination of Hill's [7] work shows that, if there is no initial disturbance, but rather a forcing that is turned on and later turned off, the solution of the forced problem can be re-expanded in terms of the linear eigenfunctions and the growth in the Tollmien-Schlichting waves calculated. Thus, even if the forcing is to lie strictly outside of the boundary layer, it must still excite an unstable Tollmien-Schlichting wave since there is little possibility that the resulting solution is orthogonal to the adjoint of the Tollmien-Schlichting wave. This is an example of forced receptivity that does not rely on any disturbance within the boundary layer proper or on any degree of non-parallelism in order to excite the unstable Tollmien-Schlichting wave. The numerical calculations presented in this paper characterize the strength of this mechanism.

That this receptivity mechanism does not *require* non-parallelism does not mean that non-parallelism can be neglected when considering receptivity. After the forcing has been turned off at a finite time, it is not physically correct to expand in terms of the initial eigenfunctions since the disturbance resulting from the forcing should be considered as the initial conditions at a higher Reynolds number. Thus, even the continuum modes that have been excited by the forcing term at the original Reynolds number could produce a Tollmien-Schlichting wave at the higher Reynolds number. However, the converse may also be true. Mathematically, this is a result of the eigenfunctions at one Reynolds number not being orthogonal to the adjoint eigenfunctions at another Reynolds number. Numerical calculations presented in this paper will show that through this mechanism, *non-parallel effects downstream of the leading edge and even into the unstable region play a major role in the receptivity problem.* In particular, Nishioka and Morkovin [9] note that for the forced receptivity problem Tollmien-Schlichting wave packets demonstrate growth far exceeding the growth of a theoretical wave packet in which it is assumed that no further seeding of the Tollmien-Schlichting waves takes place upstream of branch I of the neutral curve. Others have found such phenomena when considering naturally forced receptivity to freestream disturbances. It is also noted here that growth rates *matching* the theoretical values are found for the vibrating ribbon problem in which the continuum plays much less of a role.

The development of the theory used here for both parallel and non-parallel boundary layers is straightforward and relies on the assumption that the parallel theory is at least locally applicable for each value of the Reynolds number, *i.e.*, the same assumption used to derive the Orr-Sommerfeld equation and as a basis for analyzing the effects of non-parallelism on a single Tollmien-Schlichting wave. Assume that the governing equation (2.13) for the parallel temporal problem has been written as

$$L_R(v) = f(y,t)e^{i\omega_f t}, \tag{4.1}$$

with $f(y,0) = 0$ and $f(y,t) = 0$ for $t > T$. The frequency $\omega_f$ is considered as the primary frequency of the forcing.

Since the eigenfunctions of the Orr-Sommerfeld equation form a complete set, the solution at $t = T$

found by solving (4.1) subject to zero initial conditions and Reynolds number $R = R_1$ is

$$\breve{v}_p(y,T) = \sum_{i=1}^{N} a_i \phi_i(y,R_1) + \int_0^\infty A(k)\phi(y,k,R_1)\,dk \tag{4.2}$$

where it is chosen so that the discrete eigenfunctions are normalized to have unit energy and the continuum are also normalized with respect to the energy, *i.e.*,

$$-\frac{1}{\tilde{\gamma}^2}\int_0^\infty \phi_i^*(y,R_1)(D^2-\tilde{\gamma}^2)\phi_i(y,R_1)\,dy = 1 \tag{4.3}$$

and

$$-\frac{1}{4\delta^2\tilde{\gamma}^2}\int_{k-\delta}^{k+\delta}\int_{k-\delta}^{k+\delta}\int_0^\infty \phi^*(y,k'',R_1)(D^2-\tilde{\gamma}^2)\phi(y,k',R_1)\,dy\,dk'\,dk'' = 1. \tag{4.4}$$

If we choose $\Phi$ as the properly normalized eigenfunctions of the adjoint solution, *i.e.*,

$$-\frac{1}{\tilde{\gamma}^2}\int_0^\infty \bar{\Phi}_i^*(y,R_1)(D^2-\tilde{\gamma}^2)\phi_j(y,R_1)\,dy = \delta_{ij} \tag{4.5}$$

and

$$-\frac{1}{\tilde{\gamma}^2}\int_0^\infty \bar{\Phi}^*(y,k'',R_1)(D^2-\tilde{\gamma}^2)\phi(y,k',R_1)\,dy = \delta(k''-k'), \tag{4.6}$$

then the coefficients in (4.2) are

$$a_i = -\frac{1}{\tilde{\gamma}^2}\int_0^\infty \Phi_i^*(y,R_1)(D^2-\tilde{\gamma}^2)v_p(y,T)\,dy \tag{4.7}$$

and

$$A(k) = -\frac{1}{\tilde{\gamma}^2}\int_0^\infty \Phi^*(y,k,R_1)(D^2-\tilde{\gamma}^2)v_p(y,T)\,dy. \tag{4.8}$$

The coefficients $a_i$ are the increase in the amplitude of the Tollmien-Schlichting waves due to the forcing and $A(k)$ is the increase in the continuum modes due to forcing. Since there is no forcing for $t > T$, the evolution of the solution beyond $t = T$ is given by

$$\breve{v}(y,t) = \sum_{i=1}^{N} a_i e^{i\omega_i(R_1)(t-T)}\phi_i(y,R_1) + \int_0^\infty A(k)e^{i\tilde{\gamma}t}e^{-\iota(\tilde{\gamma}^2+k^2)(t-T)}\phi(y,k,R_1)\,dk \tag{4.9}$$

Equation (4.9) represents the exact solution for a purely parallel flow subjected to forcing. However, the boundary layer thickens as time progresses, and for a more realistic solution the effects of this must somehow be included. This thickening of the boundary layer is of course a continuous process, but insight can be gained by re-expanding the solution at $t = T$ in terms of the eigenfunctions for a larger Reynolds number. For this calculation, great care must be taken with the normalizations. First, all scalings in the $y$-direction remain as the standard scalings with $R = R_1$. The eigenfunctions and adjoint eigenfunctions for $R = R_2$ are generated by replacing $U(y)$, $U'(y)$, and $U''(y)$ in equations (2.13) and (2.14) with

$$U(y) \to U(y/\sqrt{x_0}), \qquad U'(y) \to \frac{1}{\sqrt{x_0}}U'(y/\sqrt{x_0}), \qquad \text{and} \qquad U''(y) \to \frac{1}{x_0}U''(y/\sqrt{x_0}), \tag{4.10}$$

where $\sqrt{x_0} = R_2/R_1$. The same normalization and orthogonalization relations are assumed to apply to the new set of eigenfunctions. Expanding in terms of the eigenfunctions $\phi(y,R_2)$ and $\phi(y,k,R_2)$ instead of the expansion (4.2) gives

$$\breve{v}(y,T) = \sum_{i=1}^{N} b_i \phi_i(y,R_2) + \int_0^\infty B(k)\phi(y,k,R_2)\,dk \tag{4.11}$$

with

$$b_i = -\int_0^\infty \Phi_i^*(y,R_2)(D^2-\tilde{\gamma}^2)\left(\sum_{j=1}^{N} a_j\phi_j(y,R_1)+\int_0^\infty A(k)\phi(y,k,R_1)\,dk\right)dy. \tag{4.12}$$

Taking the extreme example of $a_i = 0$, *i.e.*, the forcing producing no Tollmien-Schlichting waves at $R = R_1$, the coefficient $b_i \neq 0$ since $\Phi_i^*(y,R_2)$ is not orthogonal to $\phi(y,k,R_1)$ and $\phi_j(y,R_1)$ when $j \neq i$. This is a receptivity mechanism due to non-parallelism alone since no further disturbance within or without the boundary layer is required to initiate the gain in amplitude of the Tollmien-Schlichting wave. At first, it might be tempting to discount this route to receptivity. Upon examination on the inter-relationship between $\phi_i(y,R_1)$ and $\Phi_i(y,R_2)$ one finds

$$-\frac{1}{\tilde{\gamma}^2}\int_0^\infty \phi_i^*(y,R_2)(D^2-\tilde{\gamma}^2)\phi_i(y,R_1)\,dy \approx 1 \tag{4.13}$$

for a wide range of $R_1$ and $R_2$. It is therefore natural to assume that the orthogonality relations are also approximately preserved and that $b_i$ would automatically be quite small if $a_i = 0$. To determine whether the orthogonality relations are approximately preserved with changing Reynolds number, the entire spectrum of the Orr-Sommerfeld equation and its adjoint must be calculated along with the integrals indicated in (4.12). For the continuum, this is not a feasible undertaking. However, by numerically solving the initial value problem, this mechanism is quantifiable. The results of such a calculation are given in Section 5.2. Clearly, the analysis presented above is possible since the eigenfunctions of the Orr-Sommerfeld equation form a complete set and any function of $y$ satisfying the same boundary conditions can be expanded using this set. This leads to a more direct solution of the forced problem. Considering the component of forcing $\vec{F} = (A,B,C)$ with $\nabla\cdot\vec{F} = 0$, then equation (2.13) becomes

$$\left[\frac{\partial}{\partial t} - i\alpha U\right]\Delta\breve{v} + i\alpha U''\breve{v} = R^{-1}\Delta\Delta\breve{v} + \Delta\breve{B}, \tag{4.14}$$

with $\breve{B}(y,t)$ being the Fourier transform of the normal component of the force $\vec{F}$ that is assumed to satisfy $\breve{B}(0,t) = \breve{B}_y(0,t) = 0$. If it is also assumed that $\breve{v} = 0$ and $\breve{B} = 0$ for $t \leq 0$, then the Fourier transform in time to (4.14) gives

$$[i\bar{\omega} - i\alpha U]\,\Delta\bar{v} + i\alpha U''\bar{v} = R^{-1}\Delta\Delta\bar{v} + \Delta\bar{B} \tag{4.15}$$

where

$$\bar{v}(\alpha,y,\beta,\bar{\omega}) = \frac{1}{2\pi}\int_{-\infty}^{\infty}\breve{v}(\alpha,y,\beta,t)e^{-i\bar{\omega}t}dt. \tag{4.16}$$

Both of the time transforms $\bar{v}$ and $\bar{B}$ can be expanded in terms of the complete set of functions as

$$\bar{v}(y) = \sum_{i=1}^{N} a_i\phi_i(y) + \int_0^\infty A(k)\phi(y,k)\,dk \tag{4.17}$$

$$\bar{B}(y,\bar{\omega}) = \sum_{i=1}^{N}\beta_i(\bar{\omega})\phi_i(y) + \int_0^\infty \beta(\bar{\omega},k)\phi(y,k)\,dk. \tag{4.18}$$

Since the eigenfunctions $\phi_i(y)$, $i = 1\ldots N$ and $\phi(y,k)$, $k = (0,\infty)$ satisfy

$$i\alpha U\Delta\phi_* - i\alpha U''\phi_* + R^{-1}\Delta\Delta\phi_* = i\omega_*\Delta\phi_*, \tag{4.19}$$

there is a one-to-one correspondence between the coefficients of the expansion for $\bar{v}$ and $\bar{B}$. Thus, the exact solution is written as

$$\bar{v}(y,\bar{\omega}) = \sum_{i=1}^{N} \frac{\beta_i(\bar{\omega})}{i(\bar{\omega}-\omega_i)}\phi_i(y) + \int_0^\infty \frac{\beta(k,\bar{\omega})}{i(\bar{\omega}-\omega(k))}\phi(y,k)\,dk. \tag{4.20}$$

Then, inverting the Fourier transform in time by integrating along a contour that lies below all poles provides the coefficient of the Tollmien-Schlichting wave produced by the prescribed forcing, *i.e.*,

$$a_i = 2\pi\beta_i(\omega_i). \tag{4.21}$$

Although the temporal aspects of this result are not necessarily new (see Hill [7], Nishioka and Morkovin [9], and Crouch [4] for spatial equivalents), the dependence of this receptivity factor on the vertical profile of the divergence free component of the inhomogeneous terms is new. Some clarification of the temporal results implied by (4.21) is necessary to put the calculations that follow into context. First, the non-zero Tollmien-Schlichting wave generated by forcing is not the result of a true mathematical resonance but instead is the normal response of the solution of the homogeneous linear system to an initial value problem with an inhomogeneity. If forcing were to be of a single real frequency, $\omega_f$ say, started at $t = \infty$ instead of $t = 0$, then $\beta_i(\omega)$ is a delta function, and the evaluation at the complex frequency $\omega_i$ of the $i$th Tollmien-Schlichting wave is identically zero. However, causality is crucial to the calculations that follow. For single real frequency forcing starting at $t = 0$, $\beta_i(\omega)$ has a simple pole at $\omega_f$. It is the smallness of the growth rate, *i.e.*, the imaginary part of $\omega_i$, that produces a near resonance like behavior for the initial value problem if the real frequency $\omega_f$ matches the real part of $\omega_i$ in the same manner as the near resonant behavior in the weakly damped oscillator. However, prescribing a step function forcing is not a valid model for receptivity. The step function is known to excite all frequencies (and hence a pole rather than a delta function behavior of $\beta_i(\omega)$), and it is no surprise that a Tollmien-Schlichting wave should be excited.

There is, however, a greater chance of resonance like behavior for the continuum modes of the Orr-Sommerfeld equation. First, it is recognized that $\beta_i(\omega)$ has a pole at the real frequency $\omega_f$ for any forcing with pure sinusoidal behavior for $t > t_0$ and $t_0 >> 1$, no matter how smoothly the forcing changes from a zero value at $t = 0$ to this behavior at $t = t_0$. This pole has a factor of $e^{i(\omega_f-\omega)t_0}$ which would be small for the unstable Tollmien-Schlichting waves. However, the continuum modes with $\omega(k) = \alpha + i\epsilon(\alpha^2 + k^2)$ has an imaginary part very near zero. For $R = 1000$ and $\alpha = .25$, the imaginary part of $\omega(0)$ has a value of .0000625 while the imaginary part of the unstable Tollmien-Schlichting wave has a value of .00302. Thus, if the forcing is advected with the flow, *i.e.*, $\omega_f = \alpha$, a very near resonance with the continuum should appear, just as predicted by the model problem in Section 4.

Through (4.21) it is seen that the forced problem can be directly related to an unforced initial value problem. Assuming that the forcing is written as the product $\bar{B} = \bar{r}(\omega - \omega_f)G(y)$, then the strength of the Tollmien-Schlichting wave is proportional to

$$-\frac{1}{\tilde{\gamma}^2}\int_0^\infty \Phi_i^*(y)(D^2 - \tilde{\gamma}^2)G(y)\,dy, \tag{4.22}$$

which is the coefficient of the Tollmien-Schlichting wave for the initial value problem with $\check{v}(y,0) = G(y)$. In both Salwen and Grosch and in Hill, examples are explored by replacing the Laplacian of $G$ with a delta function centered at $y = y_0$. In Salwen and Grosch this is equivalent to specifying the initial vorticity and in Hill this is equivalent to specifying the vorticity source. Since $\Phi_i^*(y)$ behaves as $e^{-\tilde{\gamma}y}$ as $y \to \infty$, one expects that the the response to a localized source in the freestream would be proportional to $e^{-\tilde{\gamma}y_0}$. However,

the results of the numerical calculations presented later do not necessarily have this property. Instead the response sometimes decreases at a rate much faster than $e^{-\tilde{\gamma} y_0}$. The discrepancy is resolved by realizing that the specification of arbitrary initial vorticity or an arbitrary vorticity source as a delta function ignores where these quantities come from and the special nature of the integral (4.22). One interpretation of the initial value problem is that the initial values are assumed to come from the solution of the flow equations at an earlier or upstream position (naturally forced receptivity). This concept is pushed upstream until it is no longer possible to ignore the leading edge effects. For this interpretation, the initial vorticity has to be consistent with a realizable velocity field and the delta function is not. The easiest way to resolve this is to specify the initial velocity and then calculate the initial vorticity from this specification. If this is done, integration by parts of (4.22) shows that there is not an $e^{-\tilde{\gamma} y_0}$ behavior of the strength of the generated Tollmien-Schlichting wave for this mode of receptivity. This is as predicted by the model problem in Section 4.

**5. Numerical Solutions of the Linear System.** For the analysis that follows, $\vec{F}$ is chosen to have a localized structure in the $y$ variable so that the effects of forcing the boundary layer at various locations are determined. Since the problem is linear, the response to these localized forces can be considered as a form of a Green's function for the problem.

The partial differential equations (2.13) and (2.14), together with the boundary conditions (2.16) at the plate and boundedness in the freestream, were solved numerically by the method of lines. This is a convenient numerical method that has has worked well in the past; other techniques are possible. The spatial derivatives were center differenced on a uniform grid and the resulting system integrated in time.

In using such an approach on an unstable system of equations in order to quantify the instability, there is always the possibility that the instability observed in the numerical solution is actually the buildup of numerical errors rather than the instability resulting from the initial conditions or the imposed forcing. This work is particularly subject to such a criticism since it is proposed that the forcing lie entirely outside of the boundary layer. However, in previous work (Lasseigne *et.al.*, 1998), numerical errors within the boundary layer did not effect the solution to the initial value problem when disturbances originating outside of the boundary layer were considered. As the center of the initial disturbance moved away from the boundary layer, tighter tolerances were necessary to keep the numerical errors that accumulate inside the boundary layer within the proper bounds. To circumvent the issue of numerical errors producing the instabilities observed in the receptivity calculations presented below, all solutions presented are subject to the initial condition

$$\breve{v} = \frac{y^2 e^{-y^2/2}}{\int_0^\infty \left(y^4 + (1/\alpha^2)\left(y^2(2-y^2)^2\right)\right) e^{-y^2}\, dy} \tag{5.1}$$

where the normalization is chosen so that the energy is unity at the initial point. This initial condition produces the quantifiable, unstable Tollmien-Schlichting wave seen in Figure (5.1) labeled by $B_0 = 0$. To this initial value problem, forcing is added in the governing equations. It is always chosen that the forcing is identically zero at $t = 0$ and increases smoothly as a function of time. Receptivity results are presented as a gain in the amplitude to this unstable Tollmien-Schlichting wave. The drawback to including an initial condition in the forced problem is that by having two disturbances in the solution, the time marching of the numerical scheme must be slower to resolve the entire solution. However, efficiency of the numerical scheme is not of issue for this work, but proper modeling is. Even at its slowest, numerical integration of the linear, temporal stability equations is considerably faster than direct numerical simulation of the spatial

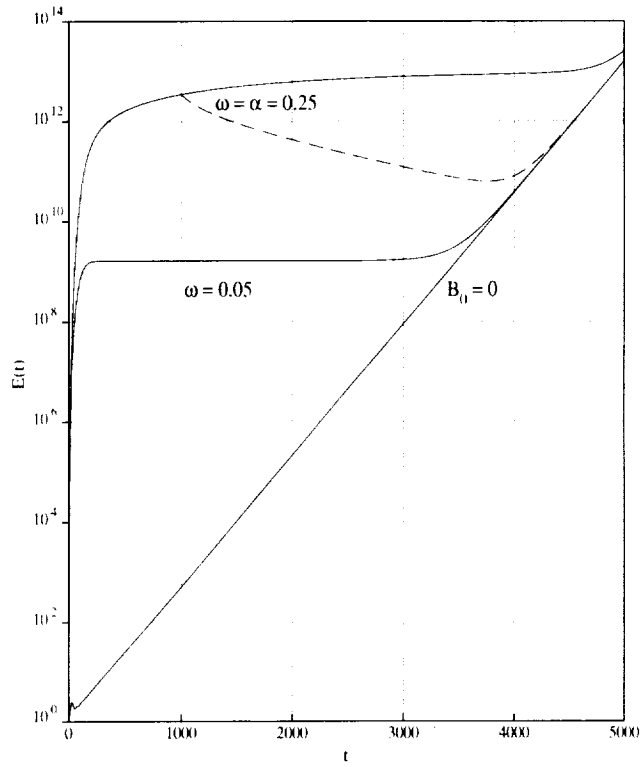


FIG. 5.1. *Response to slowly ramped single frequency forcing applied at* $y_0 = 6$. *Frequencies are* $\omega_f = 0.05, 0.25,$. *Dashed line for* $\omega_f = .25$ *with forcing stopped at* $t = 1000$.

problem. Thus, this remains an effective tool for exploring the nature of the solutions under a wide variety of conditions and guiding the more expensive numerical simulations.

**5.1. Parallel Calculations.** The first issue addressed by numerical investigation is whether or not the resonant behavior, as described in previous sections, actually occurs for the Blasius flow. To this end, the forcing function $\breve{B}$ is chosen and $\breve{A}$ and $\breve{C}$ are such that there is no forcing in the pressure equation nor in the normal vorticity equation. A general purpose function that satisfies the boundary conditions and is proportional to a delta function centered at $y_0$ in the limit as $\sigma_y \to 0$ is

$$\breve{B}(y) = B_0 r(t) e^{i\omega_f t} \frac{(y/y_0)^2 e^{-(y-y_0)^2/\sigma_y^2}}{\left(\int_0^\infty [(y/y_0)^2 e^{-(y-y_0)^2/\sigma_y^2}]^2 \, dy\right)^{1/2}} \tag{5.2}$$

The Laplacian of this function is used in the equation (2.13).

The time histories of the perturbation energy using the parameters values $B_0 = 1000$, $R = 1000$, $\alpha = \tilde{\gamma} = .25$, $\phi = 0$, $\sigma_y = .5$, and $y_0 = 6$ are shown in Figure (5.1). The forcing frequencies are $\omega_f = 0.05$ and $\omega_f = 0.25$ (for comparison, the Tollmien-Schlichting frequency is .0874). The function $r(t) = 1 - e^{-t^2/\sigma_t^2}$, $\sigma_t = 100$, provides a smooth, slow increase in the forcing. After a short transient, the constant energy curve when $\omega_f \neq \alpha$ represents the single frequency particular solution of the forced governing equations. The energy remains constant until the energy of the forced solution and the energy of the unstable Tollmien-Schlichting wave introduced by the initial conditions are of the same size. The curve with $\omega_f = \alpha$ shows greater growth in energy than the curve with $\omega_f \neq \alpha$, and this curve does not level off to a finite value. The

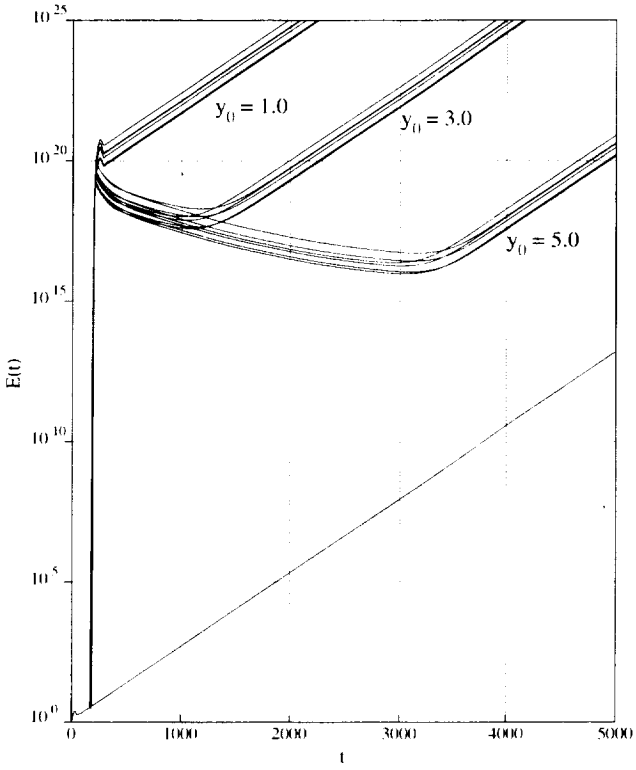


FIG. 5.2. *Response to transient forcing applied at* $y_0 = 1.0, 3.0, 5.0$. *Frequencies are* $\omega_f = 0.05, 0.25$. $\sigma_t^2 = 10, 25, 50$.

growth in energy for this resonant frequency approaches $t^2$ but is slightly less owing to damping by viscosity. This is as predicted in the inviscid analytical solutions.

In these calculations, no formal receptivity is expected since the imposed conditions are chosen to closely approximate single frequency forcing. However, according to the theory presented in Hill [7] and in Section 4, if the forcing is removed, then an unstable Tollmien-Schlichting wave *must* be generated. The only remaining question is the size of this wave. The dashed line in Figure (5.1) shows the results of smoothly removing the forcing at $t = 1000$. A significant Tollmien-Schlichting wave is not generated by forcing external to the boundary layer at this resonant frequency even though the energy of the disturbance shows tremendous growth prior to removing the forcing. Mathematically, the Tollmien-Schlichting wave must have been generated, but, since the conditions chosen ($y_0$ large and $r(t)$ smooth ) make $\beta_i(\omega)$ an extremely small number, it does not appear in Figure (5.1) .

Transient effects of forcing are explored by calculating the response to the forcing with

$$r(t) = \left(\frac{t}{t_0}\right)^2 e^{-(t-t_0)^2/\sigma_t^2}. \tag{5.3}$$

Figure (5.2) shows the time histories of the perturbation energy for eighteen cases: $t_0 = 200$, $B_0 = 10^6$, $\alpha = \tilde{\gamma} = .25$, $\phi = 0$, $\sigma_y = .5$, $\sigma_t^2 = 10, 25, 50$, $\omega_f = 0.05, 0.25$ and $y_0 = 1.0, 3.0, 5.0$. Even though the forcing is applied well outside of the boundary layer (up to $y_0 = 5$), there is an increase in the Tollmien-Schlichting wave amplitude owing strictly to this forcing. Clearly, the dominant parameter is the vertical position of the localized forcing function. This might even be unexpected since the Tollmien-Schlichting wave and its adjoint both are proportional to $\exp(-\tilde{\gamma} y_0)$ at the point of forcing. This factor cannot account for the more

that five orders of magnitude decrease seen between groups of solutions as the parameter $y_0$ varies. Also of important note in Figure (5.2) is the slow algebraic decay after cessation of the forcing when $y_0 = 5$. This is the hallmark of the response as predicted in Grosch and Salwen [10] for the continuum modes.

It is seen above that even for a single wavenumber $\tilde{\gamma} = .25$ and a single Reynolds number $R = 1000$, the strength of the receptivity response depends on a wide number of parameters forcing introduces into the problem. Using a forcing function of the form (5.2) subject to (5.3), the free parameters for this one point on the Orr-Sommerfeld diagram are: $B_0$, $t_0$, $\omega_f$, $\sigma_y$, $\sigma_t$, and $y_0$. $B_0$ is just a scaling factor in a linear problem, $t_0$ should be chosen sufficiently large such that forcing does not start immediately, and there is relatively weak dependence on $\omega_f$ and $\sigma_t$ (as compared to $y_0$). It is interesting that these two parameters do not have more of an affect considering that the width of the forcing spectrum is solely determined by them.

From the theory in Section 5, the receptivity factor is $\bar{r}(\omega_{TS} - \omega_f)$ (where $\bar{r}$ is the Fourier transform of (5.3)) times the coefficient of an eigenfunction expansion of the function $B(y)$ can be measured by extrapolating the time histories of $E(t)$ back to $t = 0$. If $a_{TS}$ is the complex coefficient of the unstable Tollmien-Schlichting wave normalized as in (4.3), then the intercept of the straight line extrapolation of the Tollmien-Schlichting energy growth seen in Figure (5.2) represents $|a_{TS}|^2$. Thus, the gain in magnitude of the quantity

$$A_{TS} = \frac{|a^i_{TS} + a^f_{TS}| - |a^i_{TS}|}{|B_0|} \tag{5.4}$$

will be referred to as the receptivity factor and used to characterize the response to the forced problem. In the limit $|B_0| \to \infty$, the contribution to the receptivity factor is from the forcing only and not from the initial condition. This coefficient has been determined for the eighteen cases included in Figure (5.2) and is tabulated in Table 1 with the Orr-Sommerfeld coefficient determined by integrating the disturbance equations with $\breve{v}(y,0) = \breve{B}(y)$ and no forcing. Also included in Table 1 is the value of $\bar{r}(\omega_{TS} - \omega_f)$ which has been determined numerically. In every case, when $\bar{r}(\omega_{TS} - \omega_f)$ is multiplied by the coefficient determined by the initial value problem, the theory agrees with the forced calculations. Additional values of $r(\omega_{TS} - Re(\omega_{TS}))$, *i.e.* forcing at exactly the frequency of the Tollmien Schlichting wave and the predicted receptivity factor are calculated and tabulated with the previous results. For these parameter values, the tuning of the forcing to match the Tollmien-Schlichting wave does not have much affect.

In the previous calculations, the function $\breve{B}$ has been specified and therefore these curves represent the case of naturally forced receptivity. In Figure (5.3), the same function was used to specify $\Delta^2\breve{B}$ and the differences in $A_{TS}$ as a function of $y_0$ is shown. As the disturbance location moves toward the freestream, the immediate generation of Tollmien-Schlichting waves have strengths proportional to $e^{-\tilde{\gamma}y}$ as was previously predicted (see Hill, 1995). The strength of immediate generation of Tollmien-Schlichting waves for the naturally forced receptivity drops off at a much faster rate as the forcing location moves toward the freestream. Thus, receptivity to turbulent disturbances which are shielded from the plate region by mean flow shear will have less than expected strength considering that the Tollmien-Schlichting waves decay as $e^{-\tilde{\gamma}y}$.

TABLE 1

*Receptivity factor for transient forcing.*

| $\sigma_t^2$ | $\omega_f$ | $y_0$ | $\bar{r}(\omega_{TS}-\omega_f)$ | Initial Value | Forced |
|---|---|---|---|---|---|
| 10 | .05 | 1 | 3.052 | $1.195*10^{1}$ | $3.647*10^{1}$ |
| 10 | .05 | 3 | 3.052 | $3.664*10^{-2}$ | $1.118*10^{-1}$ |
| 10 | .05 | 5 | 3.052 | $1.162*10^{-5}$ | $3.539*10^{-5}$ |
| 25 | .05 | 1 | 4.800 | $1.195*10^{1}$ | $5.736*10^{1}$ |
| 25 | .05 | 3 | 4.800 | $3.664*10^{-2}$ | $1.759*10^{-1}$ |
| 25 | .05 | 5 | 4.800 | $1.162*10^{-5}$ | $5.567*10^{-5}$ |
| 50 | .05 | 1 | 6.730 | $1.195*10^{1}$ | $8.041*10^{1}$ |
| 50 | .05 | 3 | 6.730 | $3.664*10^{-2}$ | $2.466*10^{-1}$ |
| 50 | .05 | 5 | 6.730 | $1.162*10^{-5}$ | $7.804*10^{-5}$ |
| 10 | .25 | 1 | 2.867 | $1.195*10^{1}$ | $3.425*10^{1}$ |
| 10 | .25 | 3 | 2.867 | $3.664*10^{-2}$ | $1.050*10^{-1}$ |
| 10 | .25 | 5 | 2.867 | $1.162*10^{-5}$ | $3.324*10^{-5}$ |
| 25 | .25 | 1 | 4.106 | $1.195*10^{1}$ | $4.906*10^{1}$ |
| 25 | .25 | 3 | 4.106 | $3.664*10^{-2}$ | $1.504*10^{-1}$ |
| 25 | .25 | 5 | 4.106 | $1.162*10^{-5}$ | $4.761*10^{-5}$ |
| 50 | .25 | 1 | 4.924 | $1.195*10^{1}$ | $5.883*10^{1}$ |
| 50 | .25 | 3 | 4.924 | $3.664*10^{-2}$ | $1.804*10^{-1}$ |
| 50 | .25 | 5 | 4.924 | $1.162*10^{-5}$ | $5.710*10^{-5}$ |
| 10 | .08744 | 1 | 3.063 | $1.195*10^{1}$ | $3.660*10^{1}$ |
| 10 | .08744 | 3 | 3.063 | $3.664*10^{-2}$ | $1.122*10^{-1}$ |
| 10 | .08744 | 5 | 3.063 | $1.162*10^{-5}$ | $3.559*10^{-5}$ |
| 25 | .08744 | 1 | 4.843 | $1.195*10^{1}$ | $5.787*10^{1}$ |
| 25 | .08744 | 3 | 4.843 | $3.664*10^{-2}$ | $1.774*10^{-1}$ |
| 25 | .08744 | 5 | 4.843 | $1.162*10^{-5}$ | $5.628*10^{-5}$ |
| 50 | .08744 | 1 | 6.849 | $1.195*10^{1}$ | $8.184*10^{1}$ |
| 50 | .08744 | 3 | 6.849 | $3.664*10^{-2}$ | $2.509*10^{-1}$ |
| 50 | .08744 | 5 | 6.849 | $1.162*10^{-5}$ | $7.958*10^{-5}$ |

**5.2. Non-parallel Calculations.** In the standard Orr-Sommerfeld approach, the value of $R$ corresponds to a specific downstream position and therefore to a particular thickness of the boundary layer. The Orr-Sommerfeld solution approach also focuses on a single mode (the least stable if $R < R_c$ or the unstable mode if $R > R_c$) which is assumed to be periodic in the streamwise direction. The basic non-parallel theory, as set out in Gaster [5], is properly considered as a problem of a spatially evolving flow. However, it appears that what is considered by this theory is the evolution of *only* one mode and not the interaction of other modes. Thus, it is still unclear how an individual disturbance, written as a sum of all eigenfunctions, evolves as the value of $R$ changes smoothly. The techniques employed here allow for the unique opportunity to measure the *linear* interactions between the eigenfunctions at two different downstream positions.

The response to forcing of the form (5.2) is shown in Section 5 to be linked to the solution of the initial value problem and this result is confirmed by the numerical experiments for the parallel problem. Therefore,

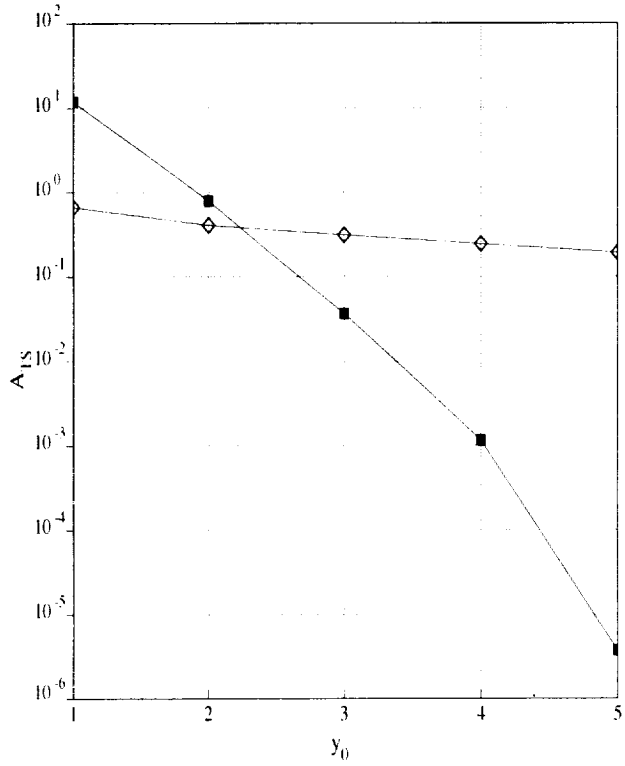


FIG. 5.3. *Difference in receptivity factor between forced modes (diamonds) and naturally-forced modes (squares) of receptivity as a function of disturbance location* $y_0$.

for the purpose of clarity, non-parallel effects are explored through a series of initial value problems, which are directly applicable to the problem of natural receptivity; the implications for the naturally forced problem can be inferred. In the spirit of using the temporal problem to explore a problem that is properly considered spatial, the Reynolds number in the disturbance equations (2.13-2.14) will be held constant and the mean flow will be amended to represent different downstream positions. The transformation is given by (4.10). The standard Orr-Sommerfeld diagram represents holding the mean flow constant ($x_0 = 1$) and the downstream evolution of a single wavelength disturbance traces a ray emanating from the origin of a $R$-$\alpha$ diagram. In this approach ($R$ is held constant and $x_0$ varied), the downstream evolution of a single wavelength disturbance traces a horizontal path in the $x_0$-$\alpha$ diagram which is shown for $R = 1000$ in Figure (5.4).

In the first series of calculations, an initial value of the form (5.2) with $r(t) = 1$ and $\omega_F = 0$ is added to the benchmark initial disturbance (5.1) and the receptivity factor $\Gamma$ is computed. Figure (5.5) shows $A_{TS}$ as a function of $y_0$. The receptivity factor is found to be decreasing slightly faster than exponentially for increasing $y_0$ as previously mentioned, but it is also shown to be an increasing function of $x_0$ (by as much as two orders of magnitude when $y_0 = 4$). When the disturbance is inside the boundary layer for all values of $x_0$ ($y_0 = 1$), the increase in receptivity factor as $x_0$ increases is about half an order of magnitude. All values shown are for the unstable region of the Orr-Sommerfeld diagram where it is possible to calculate the receptivity factor using this approach. For $y_0 = 5$ the disturbance is completely outside of the boundary layer and the increase in the receptivity factor is now several orders of magnitude (but the factor is still small). The solutions for smaller values of $x_0$ when $y_0 = 5$ could not be properly resolved using the same parameter values, but the extrapolation of the results is obvious.

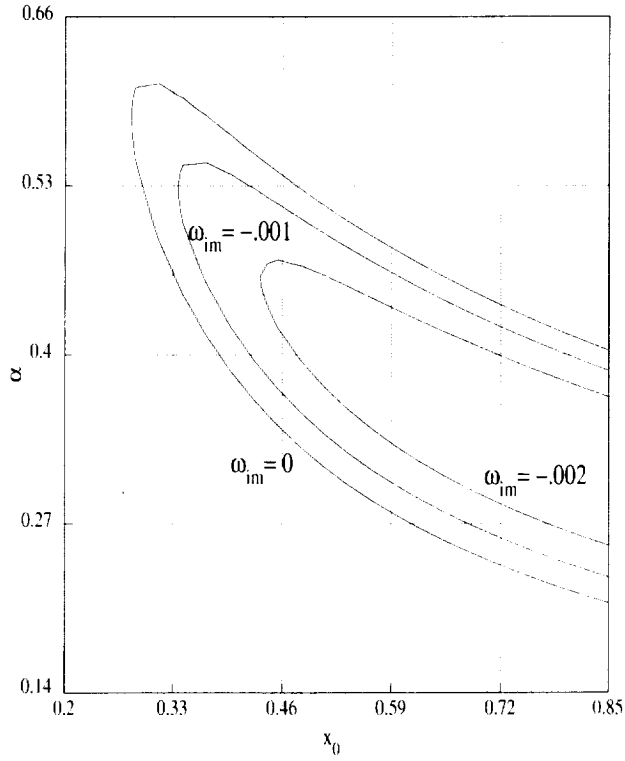


FIG. 5.4. *Growth rate contours in the $\alpha$-$x_0$ plane. Linear, parallel theory used for each value of $x_0$.*

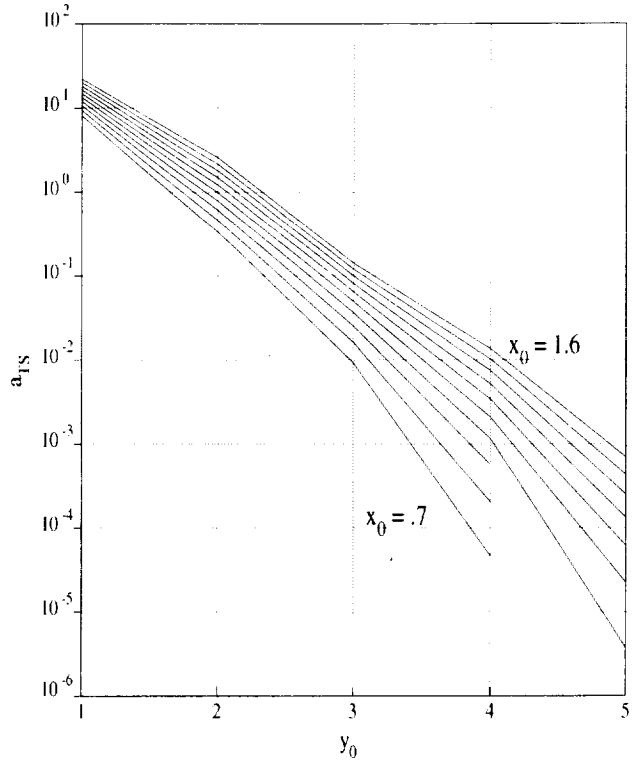


FIG. 5.5. *Effect of expanding flow on receptivity factor as a function of disturbance location $y_0$.*

In the next series of initial value problems shows order of magnitude increases in the receptivity factor as $x_0$ increases and $y_0$ large are due to the continuum modes and other Tollmien-Schlichting modes from lower value of $x_0$ feeding the Tollmien-Schlichting modes at the higher $x_0$. For $x_0 = 0.8$, an unstable Tollmien-Schlichting mode is found by calculating the solution to the governing equations for large time. This mode is then normalized to have unit energy and is used for an initial condition. Figure (5.6) shows that the variation of the Tollmien-Schlichting amplitude as $x_0$ varies from stable through the unstable region of the Orr-Sommerfeld diagram is slight. The curve for $x_0 = 0.4$ starts out with exponential decay which is to be expected if the initial condition is mostly the stable Tollmien-Schlichting wave and then decays algebraicly as expected since only the continuum is left for large times. All curves extrapolated back to $t = 0$ along the exponential part of the growth or decay give values of receptivity factors between 0.8 and 1.25. Next, the solution for initial values of the form (5.2) with $y_0 = 3$ and $x_0 = 0.8$ is calculated twice: once as is and once with an additional Tollmien-Schlichting wave added that is amplitude and phase matched to nearly cancel the instability. The results are seen in Figure (5.7) where the divergence of the solutions clearly show that the value of $a_{TS}$ for the second case is near zero. The solution using the same two initial values are calculated with $x_0 = 1$ and $x_0 = 1.2$. Surprisingly, it is seen that a majority of the Tollmien-Schlichting wave at these higher values of $x_0$ do not come from the Tollmien-Schlichting wave at $x_0 = 0.8$ but rather from the part of the solution that produces no Tollmien-Schlichting wave at $x_0 = 0.8$. The results here are rather ominous. If there is any additional disturbance in the outer edges of the boundary layer or near freestream, these disturbances feed directly into the Tollmien-Schlichting wave and will produce a growth rate greater than (sometimes very much greater than) the predicted value, *even when that predicted value accounts for all of the non-parallel effects associated with a single Tollmien-Schlichting wave.*

**6. Conclusions.** It has been shown that the techniques previously developed by the authors to investigate various aspects of the temporal stability problem can also be applied to investigate the problem of receptivity. It is shown that resonance with the continuum can occur, and this must be considered when investigating bypass mechanisms. Also shown is that the form in which the forcing function is introduced into the governing equations has great significance when determining the strength of the generated Tollmien-Schlichting wave. Perhaps most importantly, it is shown that the transfer of the solution from one downstream location to another is not one-to-one in terms of the eigenvalues, and that the continuum at one position feeds into the Tollmien-Schlichting wave at another.

## REFERENCES


[1] A. Boiko, K. Westin, B. Klingmann, V. Kozlov, and P. Alfredsson, *Experiments in a boundary layer subjected to free stream turbulence. Part 2. The role of TS-waves in the transition process*, J. Fluid Mech., (1994), pp. 219–245.

[2] W. Criminale and P. Drazin, *The initial value problem for a modelled boundary layer*, Physics of Fluids, accepted (1999).

[3] W. Criminale, T. Jackson, D. Lasseigne, and R. Joslin, *Perturbation dynamics in viscous channel flows*, J. Fluid Mech., (1997), pp. 55–75.

[4] J. Crouch, *Localized receptivity of boundary layers*, Phys. Fluids A, (1992), pp. 1408–1414.

[5] M. Gaster, *On the effects of boundary layer growth on flow stability*, J. Fluid Mech., (1974), p. 465.

[6] C. Grosch and H. Salwen, *The continuous spectrum of the Orr-Sommerfeld equation. Part 1. The spectrum and the eigenfunctions*, J. Fluid Mech., (1978), pp. 33–54.

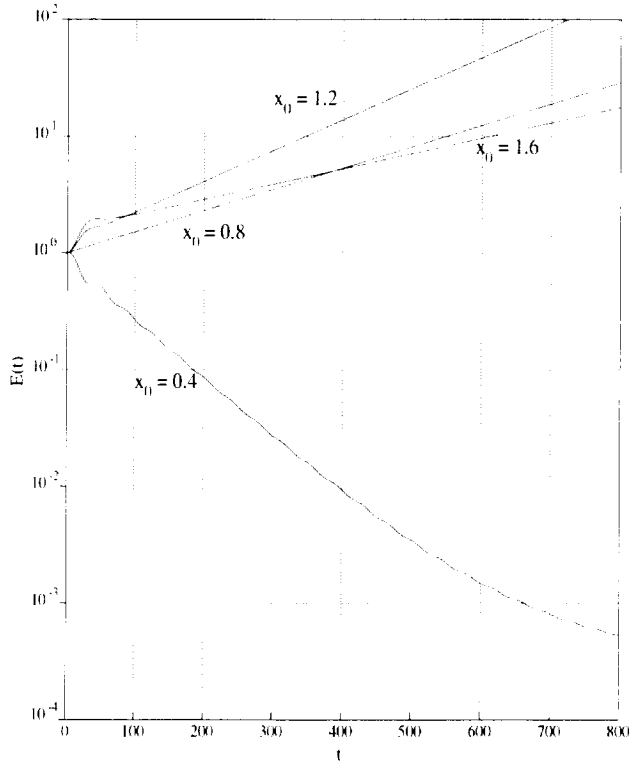


FIG. 5.6. *Responses at different downstream positions to unit Tollmien-Schlichting wave ($x_0 = 0.8$) as initial value.*


[7] D. C. HILL, *Adjoint systems and their role in the receptivity problem for boundary layers*, J. Fluid Mech., (1995), pp. 183 204.

[8] D. LASSEIGNE, R. JOSLIN, T. JACKSON, AND W. CRIMINALE, *The transient period for boundary layer disturbances*, J. Fluid Mech., (1999), pp. 351–381.

[9] M. NISHIOKA AND M. MORKOVIN, *Boundary-layer receptivity to unsteady pressure gradients: Experiments and overview*, J. Fluid Mech., (1986), pp. 219–261.

[10] H. SALWEN AND C. GROSCH, *The continuous spectrum of the Orr-Sommerfeld equation. Part 2. Eigenfunction expansions*, J. Fluid Mech., (1981), pp. 445–465.

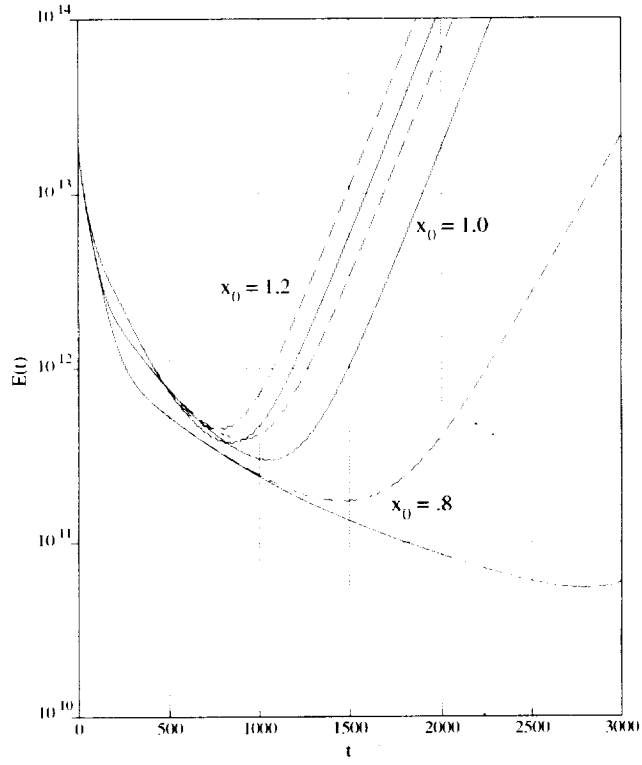


FIG. 5.7. *Response to initial conditions with and withtout Tollmien-Schlichting cancellation. Dashed lines for uncanceled response, solid lines for cancelled response.*

# REPORT DOCUMENTATION PAGE

Form Approved
OMB No. 0704-0188



| 1. AGENCY USE ONLY(Leave blank) | 2. REPORT DATE | 3. REPORT TYPE AND DATES COVERED |
|---|---|---|
| | September 1999 | Contractor Report |

**4. TITLE AND SUBTITLE**
Towards understanding the mechanism of receptivity and bypass dynamics in laminar boundary layers

**5. FUNDING NUMBERS**
C NAS1-97046
WU 505-90-52-01

**6. AUTHOR(S)**
D.G. Lasseigne, W.O. Criminale, R.D. Joslin, and T.L. Jackson

**7. PERFORMING ORGANIZATION NAME(S) AND ADDRESS(ES)**
Institute for Computer Applications in Science and Engineering
Mail Stop 132C, NASA Langley Research Center
Hampton, VA 23681-2199

**8. PERFORMING ORGANIZATION REPORT NUMBER**
ICASE Report No. 99-37

**9. SPONSORING/MONITORING AGENCY NAME(S) AND ADDRESS(ES)**
National Aeronautics and Space Administration
Langley Research Center
Hampton, VA 23681-2199

**10. SPONSORING/MONITORING AGENCY REPORT NUMBER**
NASA/CR-1999-209553
ICASE Report No. 99-37

**11. SUPPLEMENTARY NOTES**
Langley Technical Monitor: Dennis M. Bushnell
Final Report
To be submitted to the Journal of Fluid Mechanics.

**12a. DISTRIBUTION/AVAILABILITY STATEMENT**
Unclassified–Unlimited
Subject Category 34
Distribution: Nonstandard
Availability: NASA-CASI (301) 621-0390

**12b. DISTRIBUTION CODE**

**13. ABSTRACT** *(Maximum 200 words)*

Three problems concerning laminar-turbulent transition are addressed by solving a series of initial value problems. The first problem is the calculation of resonance within the continuous spectrum of the Blasius boundary layer. The second is calculation of the growth of Tollmien-Schlichting waves that are a direct result of disturbances that only lie outside of the boundary layer. And, the third problem is the calculation of non-parallel effects. Together, these problems represent a unified approach to the study of freestream disturbance effects that could lead to transition. Solutions to the temporal, initial-value problem with an inhomogeneous forcing term imposed upon the flow is sought. By solving a series of problems, it is shown that:

- A transient disturbance lying completely outside of the boundary layer can lead to the growth of an unstable Tollmien-Schlichting wave.
- A resonance with the continuous spectrum leads to strong amplification that may provide a mechanism for bypass transition once nonlinear effects are considered.
- A disturbance with a very weak unstable Tollmien-Schlichting wave can lead to a much stronger Tollmien-Schlichting wave downstream, if the original disturbance has a significant portion of its energy in the continuum modes.

**14. SUBJECT TERMS**
boundary layer, receptivity

**15. NUMBER OF PAGES**
31

**16. PRICE CODE**
A03

| 17. SECURITY CLASSIFICATION OF REPORT | 18. SECURITY CLASSIFICATION OF THIS PAGE | 19. SECURITY CLASSIFICATION OF ABSTRACT | 20. LIMITATION OF ABSTRACT |
|---|---|---|---|
| Unclassified | Unclassified | | |